

Continuous loading of cold atoms into a Ioffe-Pritchard magnetic trap

Piet O Schmidt, Sven Hensler, Jörg Werner, Thomas Binhammer, Axel Görlitz and Tilman Pfau

5. Physikalisches Institut, Universität Stuttgart, Pfaffenwaldring 57, D-70550 Stuttgart

E-mail: P.Schmidt@physik.uni-stuttgart.de

Abstract. We present a robust continuous optical loading scheme for a Ioffe-Pritchard (IP) type magnetic trap. Atoms are cooled and trapped in a modified magneto-optical trap (MOT) consisting of a conventional 2D-MOT in radial direction and an axial molasses. The radial magnetic field gradient needed for the operation of the 2D-MOT is provided by the IP trap. A small axial curvature and offset field provide magnetic confinement and suppress spin-flip losses in the center of the magnetic trap without altering the performance of the 2D-MOT. Continuous loading of atoms into the IP trap is provided by radiative leakage from the MOT to a metastable level which is magnetically trapped and decoupled from the MOT light. We are able to accumulate 30 times more atoms in the magnetic trap than in the MOT. The absolute number of 2×10^8 atoms is limited by inelastic collisions. A model based on rate equations shows good agreement with our data. Our scheme can also be applied to other atoms with similar level structure like alkaline earth metals.

PACS numbers: 32.80Pj, 42.50Vk

Submitted to: *J. Opt. B: Quantum Semiclass. Opt.*

1. Introduction

Cold atomic gases have proven to be a useful tool for a wide variety of fundamental experiments in physics including Bose-Einstein condensation (BEC) [1] and atom interferometry [2]. The preparation of ultracold atomic samples for experiments in magnetic traps is a challenging task involving multi-step cooling and trapping procedures. The starting point is usually a magneto-optical trap (MOT) [3]. Transferring the atoms from the MOT into the magnetic trap (MT) is typically accompanied by a significant loss in atom number. A crucial point of this transfer process is to match the size and position of the atomic cloud in the MOT and the MT (so called "mode matching") to obtain maximum transfer efficiency and to avoid heating [4].

We present a simple scheme for a **Continuously Loaded Ioffe-Pritchard** ("CLIP") trap, which is directly loaded from a magneto-optical trap. The CLIP trap can serve as a robust source of cold atoms for various atom optics experiments. It significantly simplifies the preparation of cold atomic samples in harmonic magnetic traps and can

be implemented for a variety of elements [5, 6]. Accumulation of atoms in the magnetic trap during operation of the MOT removes the need for a separate transfer step and allows to have more atoms than in the MOT.

Besides loading a magnetic trap, our scheme could serve as a source for magnetic waveguide experiments. A fully continuous atom laser has been on the wish list of many atomic physicists ever since the successful formation of a BEC in dilute atomic gases. In one of the most promising schemes [7], a magnetic waveguide is loaded from a MOT and evaporative cooling is performed on a continuous beam of atoms along the waveguide transforming the temporal evolution of evaporation into a spatial evolution. The mode matching of the initial MOT to the magnetic waveguide is a complicated issue [8]. Due to its continuous character, our scheme is an ideal source for this and other magnetic waveguide and atom interferometry [9, 10] experiments.

The CLIP trap is based on our previously reported continuously loaded magnetic quadrupole trap [5]. The new scheme removes the need for a transfer step from a 3D-quadrupole into an IP magnetic trap, thus greatly simplifying the preparation procedure. Another advantage is the possibility to adjust the aspect ratio in the IP trap, thus reducing the influence of the dominant density dependent loss mechanisms [5, 11]. The CLIP trap employs a modified magneto-optical trapping scheme allowing us to operate a MOT and a large volume IP trap overlapped in space and time. Atoms are magnetically trapped in a long-lived metastable state which is decoupled from the MOT light. Transfer between MOT and MT is provided by radiative leakage [12, 5, 6] from the excited state, which is populated by the MOT laser. We have implemented this scheme with atomic chromium, but also the alkaline earth metals and e.g. ytterbium are well suited [6] for that scheme and several groups are working on an implementation [13, 14].

The paper is organized as follows. In Section 2 we present the continuous loading scheme together with a discussion of the general requirements on the atomic level structure and possible implementations. In Section 3 we summarize and extend the rate equation model developed in References [5, 11] for the temperature and the accumulation of magnetically trapped atoms. The experimental setup and trapping procedure for atomic chromium is described in Section 4. Measurements of the temperature, the number of trapped atoms and the accumulation efficiency in the CLIP trap are presented in Section 5 and compared to our model. We conclude with a discussion of possible applications and extensions of our scheme in Section 6.

2. Continuous loading scheme

The basic principle of the continuous loading scheme presented here has been developed and implemented for chromium in a 3D-quadrupole magnetic trap [5]. In this paper we show that the scheme can be extended to magnetic traps of the Ioffe-Pritchard type. We will introduce the concepts of the CLIP trap with chromium. Requirements and possibilities for the implementation with other atomic species will be discussed at the end of this section.

Figure 1 shows the principle of operation. A strong dipole transition with linewidth Γ_{eg} connecting the ground state $|g\rangle$ and an excited state $|e\rangle$ allows the operation of a modified magneto-optical trap. We employ a light field configuration similar to the 2D⁺-MOT [15]: two orthogonal pairs of σ^+/σ^- -polarized laser beams cool and trap the atoms radially. An additional pair of σ^+ -polarized laser beams along the axial direction provides Doppler cooling and very weak confinement due

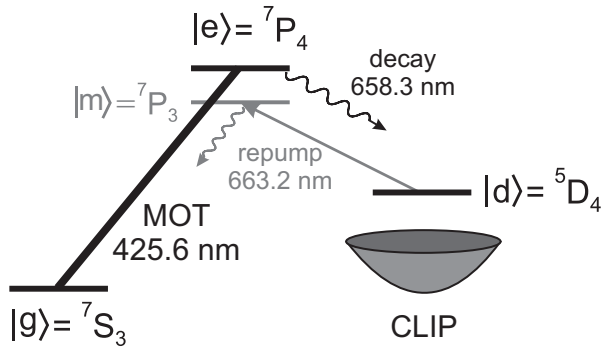


Figure 1. CLIP trap loading scheme. Shown are the relevant atomic levels and transitions for the implementation in ^{52}Cr (black lines). The magneto-optical trap is operated by driving the fast transition from $|g\rangle$ to $|e\rangle$. Transfer between MOT and CLIP trap is provided by radiative leakage from $|e\rangle$ to $|d\rangle$. Repumping the atoms via an intermediate state $|m\rangle$ (gray lines) allows to transfer the atoms to the ground state.

to light pressure forces [16, 17]. For simplicity, in the following we will refer to our configuration as "MOT", although we actually mean the modified setup just described. The radial magnetic field gradient needed for the 2D-MOT is provided by the Ioffe-Pritchard trap. The magnetic field configuration for the latter consists in radial direction (x, y) of a 2D-quadrupole with magnetic field gradient B' supporting the atoms against gravity. In axial direction (z), magnetic confinement is provided by a curvature field B'' [18]. Along the same direction, a small magnetic offset field B_0 prevents Majorana spin-flip losses [19].

The cycling transition used for the chromium MOT is not closed. Atoms can undergo spontaneous emission to a long-lived metastable state, denoted $|d\rangle$ in Figure 1, at a rate Γ_{ed} . This radiative leakage is the loading mechanism for the magnetic trap. Atoms in a low field seeking magnetic substate of the $|d\rangle$ -state manifold can be magnetically trapped in the field of the IP trap. While operating the MOT, atoms spontaneously decay to the metastable level and accumulate in the MT. The branching ratio Γ_{eg}/Γ_{ed} has to be much larger than 1 to provide cooling in the MOT before the atoms are transferred into the MT. In chromium, the branching ratio $\Gamma_{eg}/\Gamma_{ed} \approx 250000$ is rather high, thus limiting the loading rate into the CLIP trap (see Section 3.1 below). Additional optical pumping to state $|m\rangle$ would allow a much higher loading rate due to a branching ratio of only $\Gamma_{mg}/\Gamma_{md} \approx 5200$ and will be implemented in future experiments. Simultaneous operation of a MOT and a MT is only possible if the magnetic field gradient required for magnetic trapping is compatible with the MOT. Chromium with $6 \mu_B$ (Bohr magnetons) is easily supported against gravity for magnetic field gradients around 5-10 G/cm, which are typical gradients for operating a MOT with an atom having a linewidth of ~ 5 MHz.

In general, there are few requirements on the atomic species properties for an implementation of the CLIP trap scheme: (i) The atoms need to be laser-coolable to operate a MOT. (ii) A long-lived magnetically trappable state decoupled from the MOT light must exist. (iii) A dissipative transfer mechanism between MOT and metastable atoms is needed. (iv) The MOT should operate at magnetic field parameters required to trap the metastable atoms.

We will briefly discuss each of these points and possible implementations of the

continuous loading scheme for two other atomic species: rubidium as a representative of the alkali metals and strontium for the earth alkali metals.

Requirement (i) seems obvious and is met by most atomic species used in atom optics experiments, although some restrictions may apply (see below). Besides metastable states, also hyperfine states with a sufficiently large separation from the states used for the MOT, should be utilizable to fulfill condition (ii). In ^{87}Rb , where the MOT is usually operated on the $|g\rangle \hat{=} ^5\text{S}_{1/2}, F=2 \leftrightarrow ^5\text{P}_{3/2}, F=3 \hat{=} |e\rangle$ transition, the $F=1$ hyperfine state of the ^5S manifold could serve as the magnetic trapping state $|m\rangle$. Off-resonant excitation of the $^5\text{P}_{3/2}, F=2$ state by the MOT light followed by spontaneous decay to state $|m\rangle$ serves as the loading mechanism for the magnetic trap (requirement (iii)). The loading rate can be tuned by adjusting the intensity of the MOT laser beams. At this point condition (i) puts a restriction on the actual implementation: a Rb MOT without repumping the atoms from the $F=1$ to the $F=2$ manifold has a strongly reduced efficiency. The dark SPOT-MOT [20] solves this problem by surrounding a central spot in the MOT with repumping light. Also, the operation of a MOT at magnetic field gradients required for the magnetic trapping of rubidium having a magnetic moment of $0.5 \mu_B$ in the lower hyperfine state can be a problem (requirement (iv)).

A ^{88}Sr MOT for catching and precooling the atoms is typically operated between the absolute ground state $^1\text{S}_0, |g\rangle$, and the excited state $^1\text{P}_1^0$. As in chromium, this transition is not closed. Nevertheless, 8×10^7 atoms can be trapped in a Sr MOT even without repump laser [21]. Atoms can spontaneously decay via an intermediate state $^1\text{D}_2$ to the long-lived magnetic trap state $^3\text{P}_2^0, |m\rangle$ (requirements (ii) and (iii)). Additional decay channels can be closed by repumping lasers. Here, simultaneous operation of a MOT and a MT is assisted by a moderate magnetic moment of $3\mu_B$ and the spectrally broad MOT transition requiring high magnetic field gradients of 50-150 G/cm by itself (requirement (iv)). A more elaborate discussion of this trapping scheme and its variants adopted for ytterbium and other earth alkalis is given in Reference [6].

Requirement (iii) might raise the issue of reabsorption of spontaneously emitted photons by a very dense cloud of already magnetically trapped atoms. In the scheme for chromium presented here, the narrow transition $|e\rangle \leftrightarrow |d\rangle$ into the trap state is spectrally broadened by the strong MOT transition $|g\rangle \leftrightarrow |e\rangle$. The integral absorption cross section for this spin-forbidden transition to state $|e\rangle$ is determined by the small transition strength giving rise to a suppression of reabsorption by a factor of Γ_{eg}/Γ_{ed} [22, 11].

3. Model

In this section, we want to summarize and extend the model for the continuous loading scheme developed in Reference [5] and adapt it to the Ioffe-Pritchard configuration.

3.1. Number of trapped atoms

Loading of the CLIP trap is characterized by a loading rate R , proportional to the number of excited atoms in level $|e\rangle$, N_{MOT}^* , the decay rate into the metastable level Γ_{ed} , and a transfer efficiency η , giving

$$R = \eta N_{\text{MOT}}^* \Gamma_{ed}. \quad (1)$$

The maximum attainable transfer efficiency (i.e. the fraction of atoms in a magnetically trappable low field seeking state) can be estimated using a rate equation model for optical pumping. Its theoretical prediction for chromium atoms in a standard 3D-MOT is around 30% [11]. Similar values have been obtained experimentally in our CLIP trap configuration.

Accumulation of atoms in the MT is limited by loss mechanisms removing magnetically trapped atoms. We have identified two inelastic collision processes as the major loss mechanisms: (i) inelastic collisions between optically excited atoms in the MOT and atoms in the MT, characterized by a rate constant β_{ed} , and (ii) inelastic collisions between two magnetically trapped atoms with a rate constant[‡] β_{dd} . For completeness, we have also included background gas collisions at a rate γ_d , although they are negligible in our setup. The rate equation for the number of atoms in the CLIP trap, N_{MT} , reads

$$\begin{aligned} \frac{dN_{\text{MT}}}{dt} &= R - \gamma_d N_{\text{MT}} - \beta_{ed} \int_V n_e(\vec{r}) n_d(\vec{r}) dV - 2\beta_{dd} \int_V n_d^2(\vec{r}) dV \\ &= R - (\gamma_d + \gamma_{ed}) N_{\text{MT}} - 2\beta_{dd} \frac{N_{\text{MT}}^2}{V_{\text{MT}}} \end{aligned} \quad (2)$$

with

$$\gamma_{ed} = \frac{N_{\text{MOT}}^* \beta_{ed}}{V_{\text{eff}}}, \quad (3)$$

$$V_{\text{MT}} = N_{\text{MT}}^2 \left(\int_V n_d^2(\vec{r}) dV \right)^{-1}, \quad (4)$$

$$V_{\text{eff}} = N_{\text{MOT}}^* N_{\text{MT}} \left(\int_V n_e(\vec{r}) n_d(\vec{r}) dV \right)^{-1}. \quad (5)$$

Here we have introduced the loss rate γ_{ed} for collisions between MOT and MT atoms to emphasize that this process is effectively a single-atom loss for magnetically trapped atoms. In these equations, the density of atoms in the MT and in the excited state of the MOT is given by $n_d(\vec{r})$ and $n_e(\vec{r})$, respectively. The size of the effective volume V_{eff} is dominated by the larger of the two volumes V_{MOT} and V_{MT} for the magneto-optical and magnetic trap, respectively. In our experiments with chromium, we find $V_{\text{MOT}} \ll V_{\text{MT}}$, so we can approximate the effective volume with the volume of the CLIP trap $V_{\text{eff}} \approx V_{\text{MT}}$. Then, the steady state solution of Equation 2 is given by

$$N_{\text{MT}}^\infty = \frac{-(\gamma_d + \gamma_{ed}) V_{\text{MT}} + \sqrt{(\gamma_d + \gamma_{ed})^2 V_{\text{MT}}^2 + 8\beta_{dd} R V_{\text{MT}}}}{2\beta_{dd}} \quad (6)$$

Neglecting background gas collisions ($\gamma_d = 0$) and assuming saturation for the MOT transition ($N_{\text{MOT}}^* \approx N_{\text{MOT}}/2$), Equation 6 together with Equation 3 can be rewritten as an accumulation efficiency κ :

$$\kappa := \frac{N_{\text{MT}}^\infty}{N_{\text{MOT}}} = \frac{-\beta_{ed} + \sqrt{\beta_{ed}^2 + 16\beta_{dd} R V_{\text{MT}} / N_{\text{MOT}}^2}}{4\beta_{dd}}. \quad (7)$$

This equation allows an estimate of the number of atoms in the CLIP trap given the number of atoms in the MOT, N_{MOT} , and the inelastic collision properties β_{ed} and β_{dd} .

[‡] Each inelastic collision event removes two atoms from the trap. Therefore the loss rate in the differential equation for the number of atoms in the trap is twice the inelastic collision rate.

The inelastic processes limit the achievable density in the magnetic trap (Equation 2) and therefore the number of accumulated atoms. Increasing the magnetic trapping volume therefore leads to accumulation of more atoms. This is one of the main advantages of using the Ioffe-Pritchard trap over a 3D-quadrupole trap: independent control of the trapping field parameters in radial and axial direction allows increasing the magnetic trapping volume without degradation of the MOT performance.

3.2. Temperature

The temperature of the atoms in the magnetic trap is determined by the initial temperature in the MOT (T_{MOT}) and the shape of the trapping potentials [5, 11]. Assuming the MOT to be much smaller than the MT, loading occurs at the center of the magnetic trap where the atoms have only kinetic but no potential energy. In the new trapping potential the initial kinetic energy is distributed between final kinetic and potential energy according to the Virial theorem. The trapping potential in the CLIP trap is harmonic in axial and linear in radial direction, whereas the MOT is harmonic in all three dimensions. Therefore, in an ideal situation, one would expect the atoms in the CLIP trap to have $\frac{1}{2}$ and $\frac{1}{3}$ of the MOT temperature in axial and radial direction, respectively. Thermalization should result in a mean final temperature of $\sim 0.4 \times T_{\text{MOT}}$. In reality additional heating increases the temperature. One source of heating is misalignment between MOT and MT due to an imbalance in laser beam intensities. Inelastic processes like dipolar relaxation collisions [23] and fine-structure changing collisions can also contribute to heating in the MT.

It is worthwhile mentioning, that it is in fact advantageous to have the atoms in the MT not too cold if a maximum number of atoms is desired, since a hot cloud is less dense and thus allows trapping of more atoms in the presence of density limiting inelastic losses as discussed in the previous section.

4. Experimental setup and procedure

4.1. Vacuum system and lasers

Our ultra-high vacuum system consists of two vertically arranged steel chambers connected by a 50 cm long spin-flip Zeeman slower [24]. With an inner diameter of 1.5 cm, the Zeeman slower also acts as a differential pumping stage. In the lower oven-chamber chromium is sublimated at temperatures of around 1700 K in a high temperature effusion cell. A movable metal plate operated via a mechanical feedthrough allows shutting the atomic beam on and off within 200 ms. The oven chamber is pumped by a two-stage turbo-molecular pump assembly to around 10^{-8} mbar. The upper science-chamber is pumped by an ion pump and a Ti:sublimation pump yielding a pressure in the low 10^{-11} mbar regime. We have implemented a Ioffe-Pritchard trap in the cloverleaf configuration [25]. Two reentrance vacuum windows allow the operation of the trap outside the vacuum while achieving a minimum separation of 3 cm between the cloverleaf coil assemblies. We achieve a curvature of $B'' = 116 \text{ G/cm}^2$ in axial (z) and a gradient of $B' = 150 \text{ G/cm}$ (x, y) in radial direction at 300 A current through the coils. All coils are made of hollow copper tubing and are water cooled during operation.

Cooling and trapping is performed on the ${}^7\text{S}_3 \leftrightarrow {}^7\text{P}_4$ transition of ${}^{52}\text{Cr}$ at a wavelength of 425.6 nm, a linewidth of $\Gamma_{eg} = 2\pi \times 5.02 \text{ MHz}$ and a saturation intensity

of $I_{\text{sat}} = 8.52 \text{ mW/cm}^2$. The laser light for this transition is generated by frequency doubling the output of an Ar^+ -laser pumped Ti:sapphire-laser in an external, pump beam resonant cavity using a 10 mm long Brewster cut LBO crystal. We obtain 300 mW of blue light at 1.9 W fundamental input power. The laser is actively frequency-stabilized to the cooling transition in the chromium spectrum. Doppler-free polarization spectroscopy is performed in a cold gas discharge in a chromium tube under an argon atmosphere. The laser light is split between the Zeeman slower (120 mW) and the three retroreflected MOT beams (60 mW for all three beams) with an area of 11 mm^2 each. For optimum performance of the MOT, the z beam was adjusted to have less than 10 % of the total MOT intensity. In all experiments reported here, the laser detuning was set to $\delta = \omega_{\text{laser}} - \omega_{\text{atom}} = -2\Gamma_{eg}$, unless otherwise noted.

A diode laser at 663.2 nm resonant with the ${}^5\text{D}_4 \leftrightarrow {}^7\text{P}_3$ ($|d\rangle \leftrightarrow |m\rangle$) transition provides 5 mW of repumping light in a 2 mm diameter beam. This transition has a linewidth of $\gamma_{ed} = 2\pi \times 127 \text{ 1/s}$ that is inhomogeneously broadened by the ${}^7\text{S}_3 \leftrightarrow {}^7\text{P}_4$ transition. The laser frequency is locked to a mode of an evacuated and temperature stabilized Fabry-Perot reference cavity made of Zerodur and Invar.

4.2. Experimental techniques and data evaluation

We probe the atoms using fluorescence and absorption imaging on the strong $|g\rangle \leftrightarrow |e\rangle$ transition. Before imaging, magnetically trapped atoms in the metastable $|d\rangle$ state are optically pumped to the ground state with the repumping laser. Temperature, shape and magnetic moment of the atoms are not significantly changed during repumping since only two photons are scattered by every transferred atom and the involved states ${}^7\text{S}_3$ and ${}^5\text{D}_4$ have the same magnetic moment of $6 \mu_B$. The density profile of the atomic cloud is recorded with a calibrated CCD camera and fitted with the appropriate density distribution assuming thermal equilibrium. For the magneto-optical trap the density distribution is given by a Gaussian with $1/\sqrt{e}$ radius $\sigma_x = \sigma_y$ and σ_z in radial and axial direction, respectively. The density in the magnetic trap is given by a Gaussian in axial and an exponential distribution in radial direction which is modified by gravity along the y -axis:

$$n_{\text{MT}}(x, y, z) = n_0 \exp\left(-\frac{\sqrt{x^2 + y^2}}{\xi_1} - \frac{y}{\xi_2} - \frac{z^2}{2\sigma_{z,\text{MT}}^2}\right) \quad (8)$$

with

$$\xi_1 = \frac{k_B T_{\text{MT}}}{\mu B'} \quad (9)$$

$$\xi_2 = \frac{k_B T_{\text{MT}}}{mg} \quad (10)$$

$$\sigma_z^{\text{MT}} = \sqrt{\frac{k_B T_{\text{MT}}}{\mu B''}}. \quad (11)$$

In these expressions n_0 is the peak density, k_B Boltzmann's constant, g the gravitational acceleration and μ , m and T_{MT} are the magnetic moment, the mass and the temperature of the atoms, respectively. The cloud is imaged along the x -direction onto the CCD camera. For fitting the shape of the cloud, the density distribution integrated along the imaging direction is used:

$$n_{\text{MT}}(y, z) = 2n_0 \left[\exp\left(-\frac{z^2}{2\sigma_z^{\text{MT}}}\right) - \frac{y}{\xi_2} |y| \text{K}_1\left(\frac{|y|}{\xi_1}\right) \right], \quad (12)$$

where $K_1(x)$ is the modified Bessel function of the second kind of first order. The number of atoms is determined from the integrated fluorescence or absorption recorded by the calibrated CCD camera.

In all our fits, we assume a magnetic moment of $6 \mu_B$ which is in most cases a valid approximation since the magnetic trap mainly supports the extreme Zeeman substate and the change in magnetic moment during repumping to the ground state is less than 10 % and can be safely neglected [5]. Nevertheless, accumulation of other than the extreme magnetic substates in experiments involving high magnetic field gradients or due to dipolar relaxation processes can lead to some ambiguity in the determination of the shape of the trapped cloud.

The loading rate into the magnetic trap has been determined from a measurement in which we loaded the trap for a variable time and recorded the number of atoms accumulated during that time. A linear fit to the first 0-250 ms of loading yields the loading rate. We introduce an effective loading time $\tau = N_{\text{MT}}/R$ as a measure for the losses from the trap. Strictly speaking, this definition is only valid for a single-particle loss process. Nevertheless $1/\tau$ is a qualitative measure of the trap loss. More accurately, Equation 6 should be used. We measured the temperature of the atomic ensemble by a time-of-flight measurement. In this case, we also fitted the atoms released from the magnetic trap with a gaussian density distribution which gave good results after a few ms time-of-flight.

A typical experimental sequence starts with loading the CLIP trap from the MOT at a radial gradient of 13 G/cm, an axial curvature of 11 G/cm² and an offset field close to zero. After 10 s loading, MOT and Zeeman-Slower lasers are switched off and the repumping laser is switched on for 20 ms to transfer the atoms to the ground state. The magnetic trapping fields are switched off rapidly ($< 300 \mu\text{s}$) 11 ms after repumping and - in case of absorption imaging - a homogeneous magnetic support field along the imaging axis is switched on. The expanding cloud is imaged after a variable time-of-flight.

5. Performance of the CLIP trap

In this section, we present measurements on the temperature and the accumulated number of atoms in the CLIP trap. We compare our experimental results with the model presented in Section 3 and give improved numbers for the relevant collisional properties.

5.1. Temperature

We have measured the temperature of the magneto-optical and magnetic trap for different light-shift parameters $(I/I_{\text{sat}})/(|\delta|/\Gamma_{eg})$. We observed ratios between the temperature in the MT and in the MOT down to 0.35. For one set of parameters this can be seen in Figure 2. This value is in agreement with the ratio predicted from the model described in Section 3.2. Off-center loading of the MT, the finite size of the MOT and additional heating mechanisms (see Section 3.1) increase the temperature achieved in the magnetic trap and therefore lead to a deviation from the model especially at low temperatures.

One of the major advantages of the Ioffe-Pritchard trap over a 3D-quadrupole trap is the finite offset field at the center of the trap, preventing atom loss due to Majorana spin-flips for cold atomic clouds. For the radial trapping parameters in the

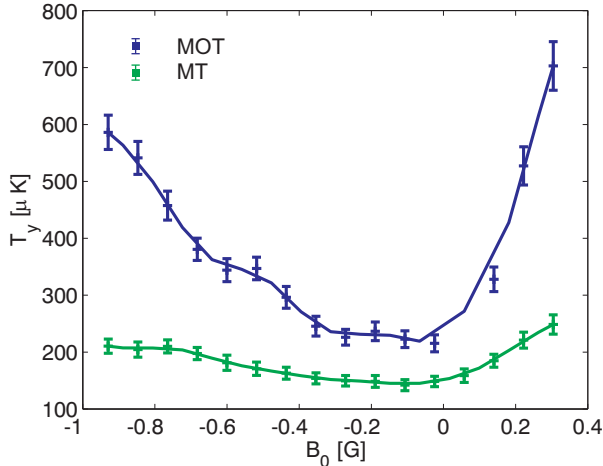


Figure 2. Radial temperature of the atoms in the MOT (black) and MT (gray) for different axial magnetic offset fields.

CLIP trap, an offset field as low as 40 mG reduces the spin-flip rate to below 0.1 1/s [19]. We observed lifetimes of more than 25 s in the CLIP trap even for negative offset fields. Although we are not limited by Majorana spin-flips while loading the CLIP trap, a small positive offset field prevents atom loss during the subsequent compression of the Ioffe-Pritchard trap.

The influence of an axial magnetic field consisting of the small offset field and the curvature field of the magnetic trap on the cooling performance in the MOT is an important aspect [26, 27, 28]. In Figure 2 we measured the radial temperature of the MOT and the MT for different axial magnetic offset field strengths. As expected, we observe a temperature minimum around zero magnetic offset field. The number of atoms in the MOT is constant over the range of magnetic fields shown in Figure 2. For negative offset fields, the MOT temperature increases only at large magnetic fields, whereas positive offset fields lead to a strong degradation of the cooling efficiency of the MOT. For optimum performance, a magnetic field strength approaching zero results in a temperature close to the minimum achievable temperature in the MOT, while at the same time preventing Majorana spin-flip losses during subsequent compression of the trap.

In summary, we observed a minimum temperature of 140 μ K in the magneto-optical and 100 μ K in the magnetic trap for low MOT light intensities and large detunings. An axial offset field close to zero does not degrade the MOT performance. We optimized the loading of our CLIP trap to achieve a maximum number of accumulated atoms at the cost of minimal temperature, thus operating the MOT at high laser light intensities and a detuning of -2Γ . Subsequent compression of the IP trap is followed by a Doppler cooling stage which results in a temperature close to the Doppler temperature independent of the initial temperature [29]. Using this preparation scheme, the figure of merit for loading the CLIP trap is reduced to the number of atoms, thus greatly simplifying adjustment and daily operation.

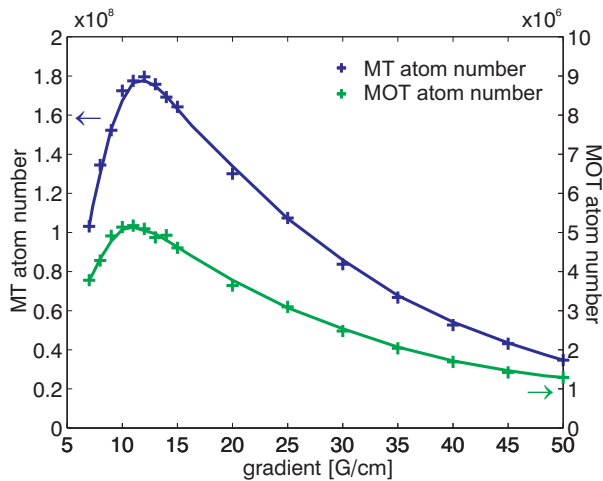


Figure 3. Steady state number of atoms in the MOT (gray) and in the CLIP trap (black) for different radial magnetic field gradients. The lines are 3-point moving averages of the data to guide the eye. Note the different scale for the number of atoms in the MOT and in the MT.

5.2. Number of atoms

In this section, we present experimental results on the number of atoms accumulated in the CLIP trap as a function of the trap parameters. We show that the steady state number of atoms is very robust against moderate magnetic field variations and demonstrate the advantages of using a Ioffe-Pritchard trap instead of a 3D-quadrupole trap. By determining independently the loading rate into the CLIP trap and the number of trapped atoms in the MOT and the MT, we are able to explain our findings qualitatively. A fit of the model developed in Section 3.1 to the experimental data results in a more accurate determination of the collision parameters responsible for trap loss than previously reported [5].

In Figure 3, we have plotted the number of atoms in the MOT and the steady state number of atoms accumulated in the CLIP trap for various radial field gradients while keeping all other trapping parameters at their optimum values. The measured volume of the magnetic trap decreases almost linearly with increasing gradient from $14 \times 10^{-3} \text{ cm}^3$ to $4 \times 10^{-3} \text{ cm}^3$. Due to an unusually high inelastic excited state collision rate for chromium [30, 11], the number of atoms in the MOT is density limited to around 5×10^6 . The number of atoms in the MT exhibits a maximum around 13 G/cm. To either side, a decrease in atom number coincides with a reduced MOT performance and thus a reduced loading rate (see Equation 1). This situation is comparable to changing the gradient of a 3D-quadrupole trap [5]: both, magnetic and magneto-optical trap are affected by a change in gradient. This can be seen more clearly in the loading rate and time measurement presented in Figure 4. The loading rate closely follows the number of atoms in the MOT for high gradients and decreases even more steeply for low gradients. This behaviour is an indication for a degradation in loading efficiency due to position mismatch between MOT and MT. The inverse of the effective loading time τ , which takes into account inelastic collisions, is a measure for the loss rate from the magnetic trap (see Section 4.2). Therefore the observed increase in effective loading time for low gradients in Figure 4 resembles a decreased

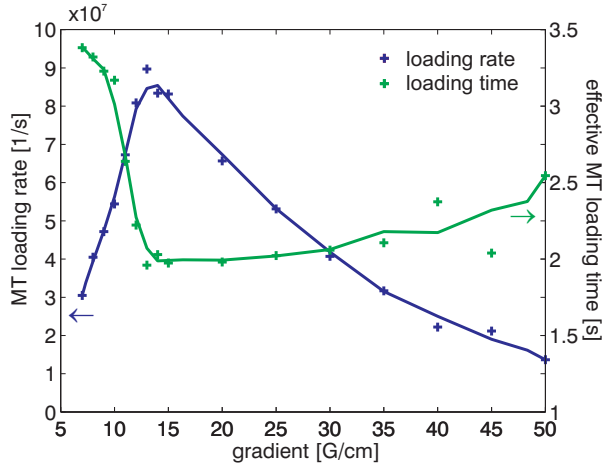


Figure 4. Loading rate into the CLIP trap (black) and effective loading time (gray) for different radial magnetic field gradients. The lines are 3-point moving averages of the data to guide the eye.

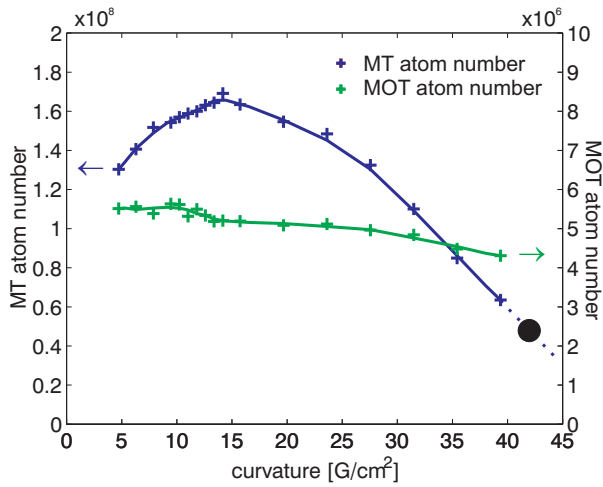


Figure 5. Steady state number of atoms in the MOT (gray) and in the CLIP trap (black) for different axial magnetic field curvatures. The filled black circle shows a typical 3D-quadrupole trap having a volume that corresponds to the volume of an IP trap with the indicated curvature. The lines are 3-point moving averages of the data to guide the eye. Note that the vertical scales are identical to Figure 3.

loss from the CLIP trap originating from a reduced number of atoms in the MOT and an increase of the trapping volume (see Equations 2 and 3).

For high gradient fields, we observe a small rise in the effective loading time. At this point the number of atoms in the magnetic trap decreases faster than the trapping volume, thus the density in the CLIP trap decreases. This leads to a slight reduction in the inelastic loss rates and therefore an increase in loading time.

The situation shown in Figures 5 and 6 is different. Here, we have changed the axial curvature and recorded the number of atoms in the MOT and the CLIP

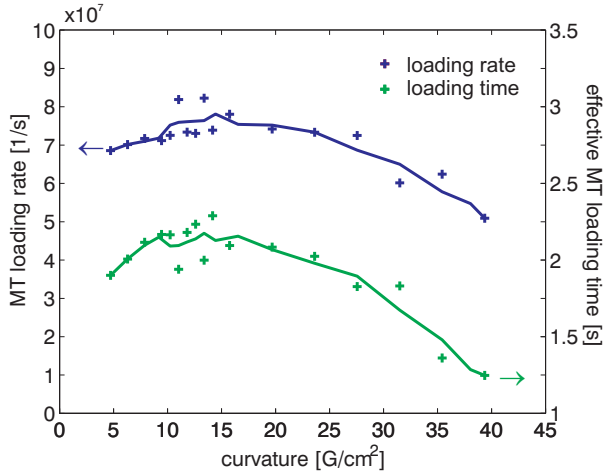


Figure 6. Loading rate into the CLIP trap (black) and effective loading time (red) for different axial magnetic field curvatures. The lines are 3-point moving averages of the data to guide the eye. Note that the vertical scales are identical to Figure 4.

trap as well as the effective loading time and rate. The volume of the magnetic trap is approximately inversely proportional to the applied curvature field, ranging from 14×10^{-3} to 3.9×10^{-3} cm^3 thus covering essentially the same range as for the gradient measurements. For comparison, we have marked in Figure 5 the equivalent curvature of a typical 3D-quadrupole trap having a volume corresponding to the volume in the CLIP trap. Whereas in Figure 3 the MOT performance is strongly affected by the radial gradient, in Figure 5 only a weak dependence of the number of atoms in the MOT on the curvature field is observed (note that the vertical axis scales in both Figures are identical). Consequently, the loading rate in Figure 6 is also constant to within 30 %. In this situation, the number of atoms accumulated in the CLIP trap is limited mainly by inelastic loss processes. This becomes evident from the decrease in the effective loading time (i.e. the increase in loss) in the high curvature regime shown in Figure 6. At very low curvatures reduced axial confinement, apparent in the reduced effective loading time, and probably misalignment between MOT and MT, noticeable in a slightly reduced loading rate, are responsible for a lower number of atoms in the CLIP trap. More accurate alignment of the MOT at low curvature fields should allow a constant loading rate at its maximum value even at low curvature fields. Such a configuration would be useful for continuous loading of a magnetic waveguide.

We achieved a maximum number of 2×10^8 atoms in the CLIP trap at a loading rate of 10^8 atoms/s for optimum trapping parameters of $B' = 12.5$ G/cm for the radial gradient, $B'' = 10.5$ G/cm² for the axial curvature and an axial offset field close to zero. This is about three times the number of atoms trapped previously in a 3D-quadrupole trap under comparable loading conditions.

The data presented in Figures 4 and 6 indicates that the effective loading time is limited to around 2 s due to inelastic collisions. We have determined the magnitude of the two major loss mechanisms by fitting the simplified rate equation model from Equation 7 to the gradient and curvature data from Figures 3 and 5. The result is shown in Figure 7, where we have plotted the accumulation efficiency $\kappa = N_{\text{MT}}/N_{\text{MOT}}$

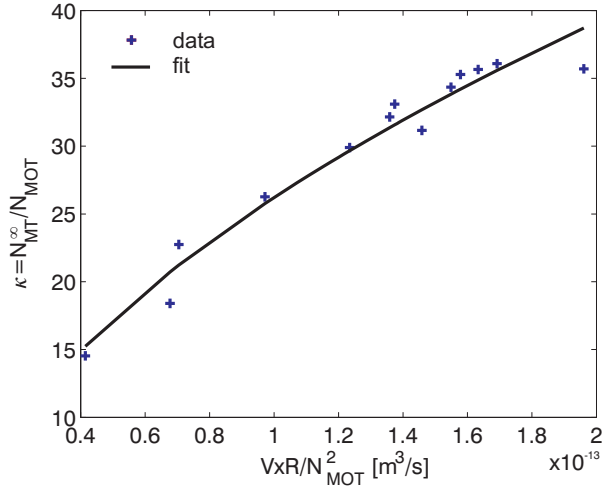


Figure 7. Accumulation efficiency into the CLIP trap versus transfer rate divided by the density of excited MOT atoms. The line is a least square fit to the data.

versus $R V_{\text{MT}} / N_{\text{MOT}}^2$. The line is a least square fit of Equation 7 to the data with β_{dd} and β_{ed} as fitting parameters. For the fit we have neglected the low gradient and curvature data points in which other loss mechanisms dominate. Since both loss rates scale with the volume of the magnetic trap, the fitting parameters are strongly correlated resulting in the large statistical uncertainty for each parameter. We obtain $\beta_{ed} = 6(9) \times 10^{-10} \text{ cm}^3/\text{s}$ for inelastic collisions between MOT atoms in the excited state and magnetically trapped atoms and $\beta_{dd} = 1.3(5) \times 10^{-11} \text{ cm}^3/\text{s}$ for inelastic collisions between atoms in the CLIP trap. Systematic errors, mainly from the determination of the densities, reduce the accuracy of the given values to within a factor of 2. These more accurate results improve the order of magnitude rates reported previously [5]. An independent measurement of β_{dd} was performed by observing the decay of magnetically trapped atoms in the $^5\text{D}_4$ state and fitting a rate equation including single- and two-atom loss processes to the data. The experimental situation in the decay measurement is different from the accumulation measurement, where only the steady state atom number is recorded. Other processes not included in our model, like e.g. dipolar relaxation [23] and variations in temperature and magnetic substate distribution of the cloud during the decay process make a comparison difficult. Nevertheless, the obtained value of $\beta_{dd} = 3.8(4) \times 10^{-11} \text{ cm}^3/\text{s}$ is close to the value from the fit to the accumulation efficiency.

6. Conclusion

We have presented a continuous optical loading scheme for ultracold atoms from a magneto-optical trap into a Ioffe-Pritchard magnetic trap. We achieved temperatures below $100 \mu\text{K}$, a loading rate of up to 10^8 atoms/s and 2×10^8 atoms accumulated in the magnetic trap in our implementation for chromium atoms. The loading rate is limited by the small number of atoms trappable in a chromium MOT [30, 11] and the small decay rate Γ_{ed} into the metastable trap state. We plan to increase the loading rate by optically pumping the atoms via another fine structure level of the excited state

that has a higher decay rate into the trap state. Two major loss mechanisms limit the number of atoms in the magnetic trap: inelastic collisions among excited state atoms in the MOT and magnetically trapped atoms and inelastic collisions between atoms in the magnetic trap [5]. We have presented a model for the steady state number of atoms in the magnetic trap that is in good agreement with our experimental data. From a fit of the model to the data we could determine the loss rates for the two inelastic density limiting processes to be $\beta_{ed} = 5 \times 10^{-10} \pm 45 \%$ cm³/s and $\beta_{dd} = 1.3 \times 10^{-11} \pm 17 \%$ cm³/s for collisions between MOT and MT atoms and between MT atoms, respectively. Independent control of the radial and axial trapping fields in the Ioffe-Pritchard trap allowed us to accumulate more atoms in the MT by increasing the volume of the trap without losing confinement or deteriorating MOT performance. The inelastic loss in the metastable trap state in chromium requires repumping the atoms to the ground state for subsequent experiments.

We use the CLIP trap loading scheme as a starting point for further cooling sequences. Consecutive Doppler cooling of ground state atoms in a compressed IP magnetic trap reduces the figure of merit for loading of the MT to the number of atoms instead of phase space density [29]. Radio frequency induced evaporative cooling towards a Bose-Einstein Condensate of chromium atoms is currently under investigation.

Our experiments at low axial confinement (Figures 5, 6) show that continuous loading of a magnetic waveguide should be possible. In that case, slightly tilting the trap would allow the atoms to escape the trapping region resulting in a continuous flux of 10^8 magnetically trapped ultracold atoms per second in the case of chromium.

Another possibility of accumulating orders of magnitudes more atoms would be to extend the Ioffe-Pritchard configuration. For example the combination of a tilted magnetic waveguide with magnetic or optical endcaps could serve as a large volume accumulation reservoir and prolong the loading time.

The continuously loaded Ioffe-Pritchard trap presented here is not limited to chromium. Atoms like e.g. the earth alkalis and ytterbium with a large natural linewidth allow high gradients for operating the MOT, thus enabling magnetic trapping at the same time. Besides this feature, the earth alkalis have a level structure which is especially well suited for the continuous loading scheme presented here or variations of it [6].

Acknowledgments

This work was funded by the Forschergruppe "Quantengase" der Deutschen Forschungsgemeinschaft and the European Research and Training Network "Cold Quantum Gases" under Contract No. HPRN-CT-2000-00125. P.O.S has been supported by the Studienstiftung des deutschen Volkes.

- [1] M. Inguscio, S. Stringari, and C. E. Wieman, eds. *Bose-Einstein Condensation in Atomic Gases* (International School of Physics "Enrico Fermi", 1998).
- [2] P. R. Berman, ed. *Atom Interferometry* (Academic Press, New York, 1997).
- [3] C. G. Townsend, *et al.* Phys. Rev. A **52**, 1423 (1995).
- [4] W. Ketterle, D. Durfee, and D. Stamper-Kurn in *Proceedings of the International School of Physics - Enrico Fermi*, edited by M. Inguscio, S. Stringari, and C. Wieman p. 67 (IOS Press, 1999).
- [5] J. Stuhler, *et al.* Phys. Rev. A **64**, 031405 (2001).
- [6] T. Loftus, J. R. Bochinski, and T. W. Mossberg Phys. Rev. A **66**, 013411 (2002).
- [7] E. Mandonnet, *et al.* Eur. Phys. J. D **10**, 9 (2000).
- [8] J. Dalibard private communication (2001).

- [9] E. A. Hinds, C. J. Vale, and M. G. Boshier Phys. Rev. Lett. **86**, 1462 (2001).
- [10] E. Andersson, *et al.* Phys. Rev. Lett. **88**, 100401 (2002).
- [11] J. Stuhler *Kontinuierliches Laden einer Magnetfalle mit lasergekühlten Chromatomen* Dissertation Universität Konstanz, Lehrstuhl J. Mlynek Ufo-Verlag, Allensbach (2002).
- [12] A. S. Bell, *et al.* Europhys. Lett. **45**, 156 (1999).
- [13] T. Loftus private communication (2002).
- [14] We plan to implement this loading scheme for a different experiment with ytterbium atoms.
- [15] K. Dieckmann, R. J. C. Spreeuw, M. Weidemüller, and J. T. M. Walraven Phys. Rev. A **58**, 3891 (1998).
- [16] J. Dalibard Opt. Comm. **68**, 203 (1988).
- [17] A. P. Kazantsev, G. I. Surdutovitch, D. O. Chudesnikov, and V. P. Yakovlev J. Opt. Soc. Am. B **6**, 2130 (1989).
- [18] W. D. Phillips, J. V. Prodan, and H. J. Metcalf J. Opt. Soc. Am. B **2**, 1751 (1985).
- [19] C. Sukumar and D. Brink Phys. Rev. A **56**, 2451 (1997).
- [20] W. Ketterle, *et al.* Phys. Rev. Lett. **70**, 2253 (1993).
- [21] H. Katori, T. Ido, Y. Isoya, and M. Kutawa-Gonokami Phys. Rev. Lett. **82**, 1116 (1999).
- [22] L. Santos, F. Floegel, T. Pfau, and M. Lewenstein Phys. Rev. A **63**, 063408 (2001).
- [23] P. O. Schmidt, *et al.* *Dipolar Relaxation in ultracold Dipolar Gases*, in preparation.
- [24] A. Witte, T. Kisters, F. Riehle, and J. Helmcke J. Opt. Soc. Am. B **9**, 1030 (1992).
- [25] M.-O. Mewes, *et al.* Phys. Rev. Lett. **77**, 416 (1996).
- [26] M. Walhout, J. Dalibard, S. L. Rolston, and W. D. Phillips J. Opt. Soc. Am. B **9**, 1997 (1992).
- [27] M. Walhout, U. Sterr, and S. L. Rolston Phys. Rev. A **54**, 2275 (1996).
- [28] S. Chang, T. Y. Kwon, H. S. Lee, and V. G. Minogin Phys. Rev. A **66**, 043404 (2002).
- [29] P. O. Schmidt, *et al.* *Doppler cooling of an optically dense cloud of trapped atoms*, arXiv: quant-ph/0208129 (2002).
- [30] C. C. Bradley, J. J. McClelland, W. R. Anderson, and R. J. Celotta Phys. Rev. A **61**, 053407 (2000).